Nuclear Magnetic Resonance Study of Solvent Exchange and Nuclear Overhauser Effect of the Histidine Protons of Bovine Superoxide Dismutase†

James D. Stoesz,‡ Douglas P. Malinowski,§ and Alfred G. Redfield*

ABSTRACT: The downfield histidine imidazole N proton resonances of bovine superoxide dismutase [Lippard, S. J., Burger, A. R., Ugurbil, K., Pantoliano, M. W., & Valentine, J. S. (1977) *Biochemistry 16*, 1136] have been studied by pulsed NMR in H_2O buffer. Exchange rates with solvent and nuclear Overhauser effects (NOE), mainly with imidazole C2 and C4 protons on the same residue, have been found. In the reduced state, resonances observed (at pH 7) at 13.9 and 12.8 ppm downfield from DSS are shown to be His-41 N3 and N1 protons, respectively, by NOE to a common C2–H resonance previously identified with this residue [Cass, A. E. G., Hill, H. A. O., Smith, B. E., Bannister, J. V. & Bannister, W. H. (1977) *Biochemistry 16*, 3061] and by mutual second-order NOE. The 12.8-ppm resonance shifts upfield above pH 9.5, showing that His-41 has a pK_a of about 10.4. Protons resonating at 15.35 and 13.4 ppm are the most slowly exchanging, with similar rates ($\sim 2 \times 10^{-5}$ s^{-1} at 37 °C) and activation energies ($\sim$30 kcal/mol). They are identified with the two most buried active-site histidine residues, 44 and 69, and are both N1 coordinated to the active-site metals. The NOE of the resonance at 12.5 ppm shows that the corresponding residue is N3 coordinated. The resonance at 13.9 ppm and a broad resonance at 12.6 ppm show base-catalyzed kinetic broadening above neutral pH; the other resonances remain observable to pH 10.5. In the oxidized state, NOE established that broad resonances at 12.1 and 13.6 ppm originate from His-41. The magnitude of the NOE is used to estimate several interproton distances, and strategies for selective NOE observation are discussed.

Superoxide dismutase, an enzyme apparently ubiquitous to aerobic cells, protects these cells against the toxic effects of oxygen by catalyzing the dismutation of O_2^- to O_2 and H_2O_2 at rates near the diffusion-controlled limit. The bovine erythrocyte enzyme is a dimer made of identical subunits, each of which contains a Cu (I or II) ion and a Zn(II) ion (Fridovich, 1975). The metal atoms are about 6 Å apart and share a common ligand, His-61. The coordination about the copper is approximately square planar; the imidazole groups of His-44, His-46, and His-118 are the remaining ligands (Beem et al., 1977). The His-69, His-78, and Asp-81 side chains complete an approximately tetrahedral arrangement about the zinc ion (Richardson et al., 1975a,b). The enyzme contains two additional histidine residues, His-19 and His-41, which are not part of the active site.

Lippard et al. (1977) have studied the nuclear magnetic resonance (NMR) spectrum of bovine erythrocyte superoxide dismutase and have observed five resonances due to exchangeable protons between 12.0 and 16.0 ppm downfield of DSS which they tentatively assign as histidine NH resonances. Our work has two objectives. First, each of these resonances must be assigned to a specific histidine residue. We have accomplished this for four of the resonances using solvent exchange rate measurements, nuclear Overhauser effect (NOE)[1] data, and selective histidine C2 proton exchange. Our second goal is to characterize the environment of each proton to obtain unique, specific information on the histidine residues.

Experimental Section

Bovine copper zinc superoxide dismutase (M_r 31 500) was isolated from liver as described previously (McCord & Fridovich, 1969). NMR samples consisted of approximately 1.0 $\times 10^{-3}$ M enzyme, 0.05–0.10 M buffer, and 1.0×10^{-4} M EDTA. Buffers used were phosphate between pH 6 and 8, borate between pH 8 and 10, and carbonate above pH 10.0. Most spectra were obtained in 90% H_2O and 10% D_2O. Values of pH are uncorrected meter readings. When required, superoxide dismutase was reduced by addition of a minimum amount of solid sodium dithionite.

Exchange of the C2 proton of His-41 for deuterium was accomplished much as described previously (Cass et al., 1977a). Superoxide dismutase (1.5×10^{-3} M) was incubated in 98% D_2O, 0.05 M phosphate, and 1.0×10^{-4} M EDTA, pH 8.9 ± 0.1, at 40 °C for 4 h. After addition of HCl to lower the pH to 6.5, the sample was lyophilized and redissolved in 90% H_2O–10% D_2O buffer for further experiments.

Fourier transform proton NMR spectra in H_2O solutions were obtained on the LDB-270 spectrometer as described previously (Redfield et al., 1975). The observation pulse was a 214 pulse, which flips over the entire downfield region of the spectrum without producing a strong solvent signal and without saturating the solvent protons. Spectra are reported in parts per million downfield of DSS. Convolution difference spectra were obtained by subtracting a spectrum smoothed by performing many (about 20) three-point averages of the original data and normalized to give a flat base line.

Longitudinal relaxation rates were measured by selective saturation–recovery. The apparent relaxation time, T_{1a}, is defined as the inverse of the first-order rate of recovery from a selective saturation pulse. Our typical pulse sequence

† From the Department of Biochemistry, Brandeis University, Waltham, Massachusetts 02254 (J.D.S. and A.G.R.), and the Department of Biochemistry, Duke University Medical Center, Durham, North Carolina 27710 (D.P.M.). *Received June 15, 1979.* Supported by U.S. Public Health Service Grants GM20168 and GM10287 and by the Research Corporation. A.G.R. is also at the Physics Department and the Rosenstiel Basic Medical Sciences Research Center, Brandeis University. Contribution No. 1278 from the Department of Biochemistry, Brandeis University.

‡ National Institutes of Health Postdoctoral Fellow, 1978. Present address: Central Research, 3M Co., St. Paul, MN 55101.

§ Present address: Department of Biochemistry, University of Washington, Seattle, WA 98195.

[1] Abreviations used: NOE, nuclear Overhauser effect; NMR, nuclear magnetic resonance; EDTA, ethylenediaminetetraacetic acid; DSS, sodium 2,2-dimethyl-2-silapentane-5-sulfonate.

0006-2960/79/0418-4669$01.00/0

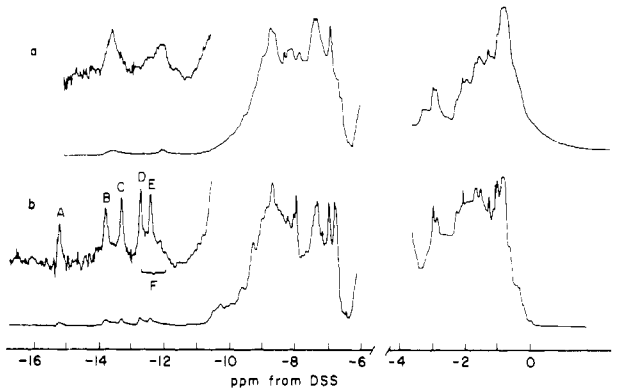

FIGURE 1: The 270-MHz ^{1}H NMR spectra of native bovine superoxide dismutase. (a) Oxidized enzyme [Cu(II),Zn(II] at 20 °C and pH 6.25; (b) reduced enzyme [Cu(I),Zn(II)] at 20 °C and pH 6.95.

consisted of a 0.1-s preirradiation pulse, whose power was set to just saturate one resonance, a variable delay time, and an observation pulse. Magnetization recovery was exponential to within error over two to three T_{1a}'s, provided only a single proton was saturated for less than 0.2 s. Transfer of water saturation experiments were performed as described previously (Stoesz et al., 1978). The pulse sequence in the NOE experiments usually consisted of a 0.1-s preirradiation pulse to saturate a proton of interest, a 1- or 2-ms field-homogeneity spoil pulse, a 2- or 3-ms spoil–recovery time, and an observation pulse. The preirradiation pulse frequency was alternated between a control frequency and the desired frequency every 2, 4, or 16 pulses; the resulting spectra were subtracted in computer memory, yielding a NOE difference spectrum free from long-term instrumental instability problems.

Results

The 270-MHz proton NMR spectra of oxidized and reduced bovine copper zinc superoxide dismutase are shown in Figure 1. As reported previously (Lippard et al., 1977), the oxidized enzyme shows two broad resonances downfield of 11 ppm, while the reduced enzyme displays five sharper resonances in this region. These peaks were tentatively assigned to histidine N protons. We label the downfield proton resonances in the reduced protein A–F, where F is a broad resonance at 12.6 ppm. Resonance F broadens as the pH is raised and is not seen above pH 7.0.

Upfield of the histidine NH resonances there are numerous peptide NH and aromatic side chain resonances. The histidine C2 and C4 protons observed between 6.0 and 9.0 ppm are of particular interest to us. These protons have been partially assigned by Cass et al. (1977a,b). Exact comparison of spectra between these previous studies and our work is difficult because of a difference in experimental conditions [50 °C and 1.0 M KCl, Cass et al. (1977b), vs. 20 °C and 0.05 M phosphate in this work]. The aliphatic region of the NMR spectrum of superoxide dismutase appears similar to that reported previously.

The pH dependence of the chemical shifts of peaks A–E in the reduced protein is reported in Figure 2. Resonances A and C show little pH dependence. Resonance B broadens noticeably as the pH is raised above 7.0 and is not observed above pH 8.0, probably because of rapid solvent exchange. Peak D shifts upfield at high pH with an approximate pK_a of 10.5, but no broadening is observed in this pH region. While the chemical shift of resonance E is independent of pH, this peak broadens as the pH is raised above 10.0. The origin of the slight upfield shift of all the resonances with increasing pH is not known.

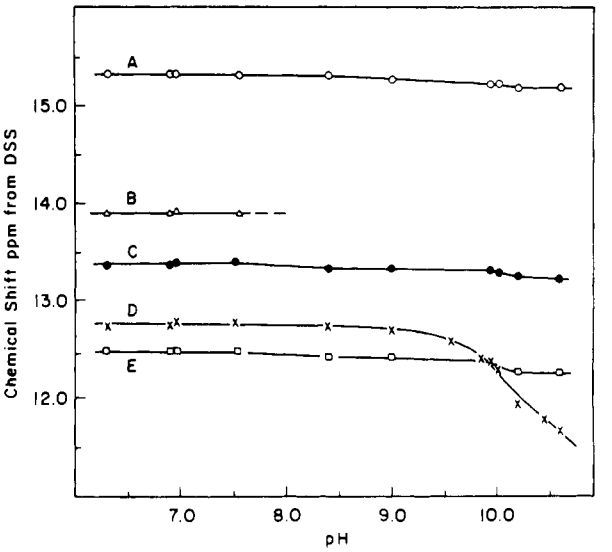

FIGURE 2: The pH dependence of the chemical shifts of resonances A–E of reduced superoxide dismutase at 20 °C. All lines are hand drawn. The titration of resonance D has a pK_a of 10.4 ± 0.3.

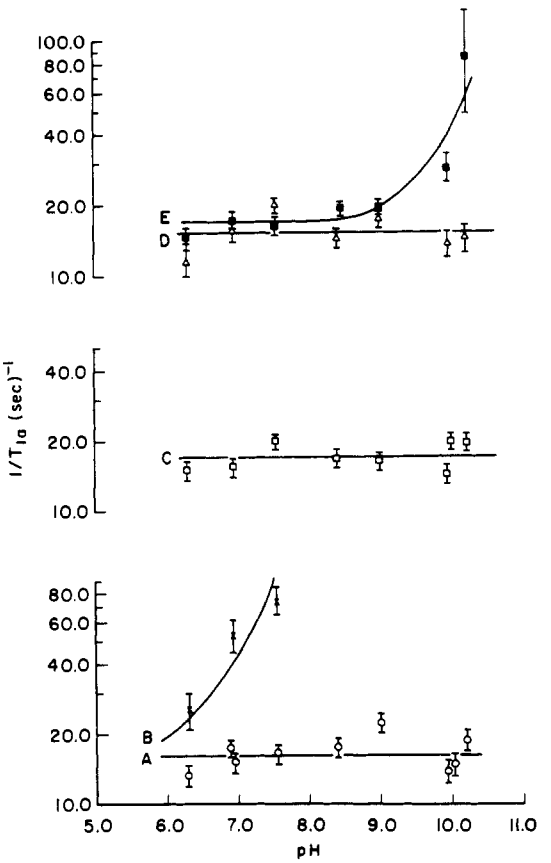

FIGURE 3: The pH dependence of the apparent longitudinal relaxation rates T_{1a}^{-1} of resonances A–E of reduced superoxide dismutase as determined by selective saturation–recovery experiments at 20 °C. The solid lines for peaks B and E were calculated from eq 1, and hydroxide-catalyzed exchange rates are shown in Table I.

The apparent longitudinal relaxation times for resonances A–E, measured by selective saturation–recovery, are reported in Figure 3. T_{1a} values for peaks A, C, and D are pH independent and are near 60 ms. Peaks B and E show strong pH dependence in T_{1a} above pH 7 and pH 10, respectively, where their line widths also increase significantly. The recoveries of peaks D and E contain a fast-relaxing component (approximately 10 ms) at pH 6.3 which can be ascribed to the broad resonance F. This peak is clearly visible at 12.6 ppm,

Table I: Chemical Exchange Rates

proton	exchange rate[a]	conditions
A	$k_{ex} = 3.0 \times 10^{-5}$ s^{-1}	pH 7.2; 37 °C
B	$k_{OH} \sim 2.5 \times 10^{8}$ L mol^{-1} s^{-1}	20 °C
C	$k_{ex} = 2.0 \times 10^{-5}$ s^{-1}	pH 7.2; 37 °C
D	$k_{ex} < 20$ s^{-1}	pH 10.2; 20 °C
D	$k_{ex} > 3 \times 10^{-3}$ s^{-1}	pH 6.6; 5 °C
E	$k_{OH} \sim 2.5 \times 10^{5}$ L mol^{-1} s^{-1}	20 °C

[a] Reported as either k_{ex}, the pseudo-first-order exchange rate, or k_{OH}, the second-order hydroxide-catalyzed exchange rate.

13 ms after the end of a preirradiation pulse which saturates the region from 11.5 to 13.5 ppm.

The longitudinal relaxation time for an exchangeable protein proton may contain contributions from several sources. Assuming no pH-dependent protein processes affect the environment, hydration, or correlation time of the protons of interest, contributions from most terms will be pH independent. These may include sources of magnetic relaxation such as nitrogen intramolecular relaxation and dipole–dipole couplings due to solvent or protein protons, as well as contributions from pH-independent chemical exchange processes which might result from H_2O-catalyzed exchange or rate-limiting conformational steps in the exchange mechanism. The major source of pH-dependent recovery will be hydroxide-catalyzed exchange. We can express this as

$$1/T_{1a} = R_1 + k_{OH}[OH^-] \quad (1)$$

where R_1 is the sum of all pH independent relaxation and exchange processes and k_{OH} is the rate constant for hydroxide-catalyzed exchange. Our observation of a pH-independent T_{1a} for peaks A and C, which exchange very slowly with water (see below), supports our contention that R_1 is pH independent. Equation 1 is able to account for the pH dependence of T_{1a} for resonances B and E; calculated values of k_{OH} are reported in Table I.

We have measured the transfer of saturation from water to resonances A–E to verify our interpretation of the T_{1a} data (Figure 4). Greater than 90% of saturation is transferred from water to resonance B at pH 7.55 and to resonance E at pH 10.2, confirming that, for these conditions, chemical exchange is dominant in the saturation–recovery mechanism for these protons. As the pH is lowered, transfer of saturation decreases as expected for hydroxide-catalyzed solvent exchange but levels off at a pH-independent value of 50–60% for both resonances. Transfer of saturation from water is observed to be pH independent at pH values less than 10.0 and is approximately 55% for resonances A and C and 35% for resonance D.

Possible causes for the substantial pH-independent transfer of saturation include (1) direct solvent cross relaxation (Glickson et al., 1976); (2) pH-independent chemical exchange, and (3) protein proton-mediated solvent cross relaxation (Stoesz et al., 1978).

Most of the histidine N protons are not in direct contact with water, making the direct solvent cross relaxation mechanism unlikely. Chemical exchange can be ruled out as a mechanism of saturation transfer for at least two peaks by the following experiment. Fully protonated protein was dissolved in D_2O at pH 6.6 and 5 °C, immediately reduced with dithionite, and examined in the NMR spectrometer. In the first spectrum, obtained at an average time of 6 min, all resonances, except A and C, had completely exchanged. Peaks A and C do not measurably exchange in 3 days at pH 6.6 and 5 °C. Raising the temperature to 50 °C caused complete exchange in several hours. The temperature dependence of the first-order solvent exchange rates for peaks A and C,

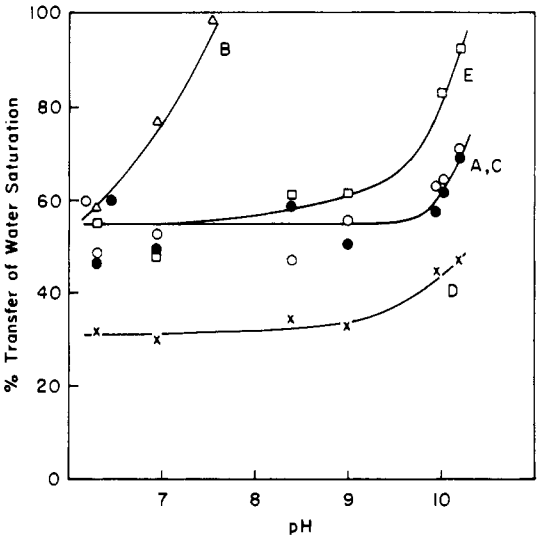

FIGURE 4: The pH dependence of the percent of transfer of water saturation to resonances A–E of reduced superoxide dismutase at 20 °C. (○) Peak A; (△) peak B; (●) peak C; (×) peak D; (□) peak E. The lines were hand drawn to fit the data. The error in each measurement is about ±10%. The increase in transfer of saturation to peaks A, C, and D above pH 10 is only marginally significant, and we have no proven interpretation for the effect. The pH dependences for peaks B and E are discussed in the text.

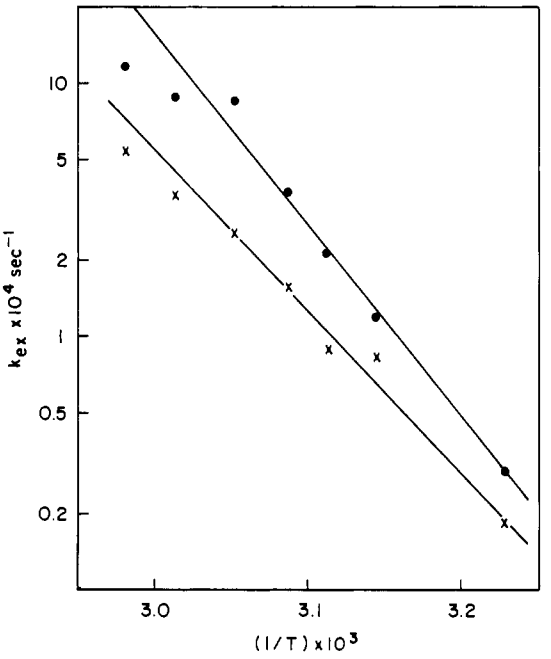

FIGURE 5: The temperature dependences of the first-order solvent exchange rates of peaks A and C at pH 7.2. (●) Peak A; (×) peak C. We estimate that the errors in the rates are ±10%. The activation energies are 34 kcal/mol for peak A and 29 kcal/mol for peak C.

measured as described above, is shown in Figure 5. Approximate rate constants or limits on rate constants for solvent exchange of all peaks are reported in Table I.

The feasibility of the remaining mechanism of saturation transfer, protein proton-mediated solvent cross relaxation, has been demonstrated as follows (Stoesz et al., 1978). (1) Saturation of water reduced the integrated intensity of the entire protein spectrum by 35–40%, indicating that spin transfer between water and the protein is quite efficient. No region or peak in the spectrum is observed to saturate substantially more or less than the average value. (2) Saturation of the resonances between 0.0 and 3.5 ppm is nearly completely transferred to the histidine NH resonances whose apparent

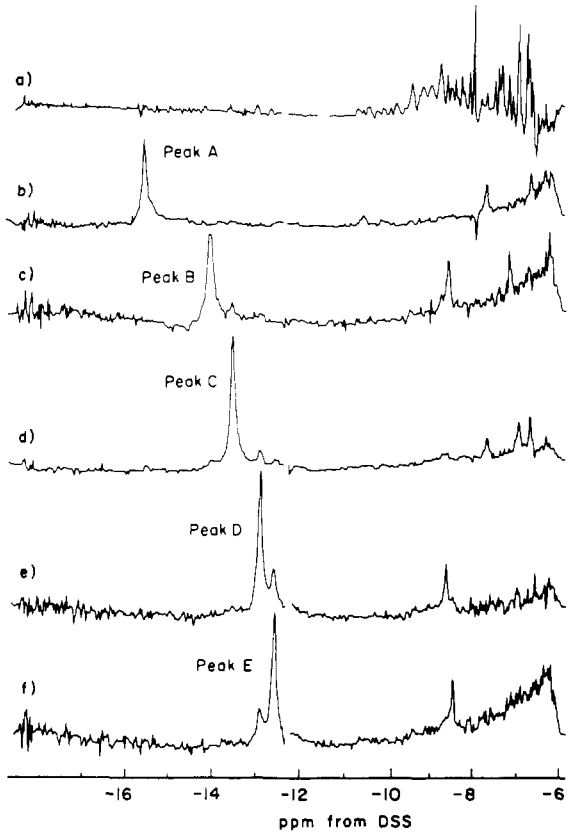

FIGURE 6: NOE difference spectra for resonances A–E of reduced superoxide dismutase at pH 6.6 and 20 °C. Experiments were performed as described in the text. Spectrum a is the convolution difference spectrum of the enzyme, and spectra b–f are difference spectra (not convoluted): (b) saturation of resonance A; (c) saturation of resonance B; (d) saturation of resonance C; (e) saturation of resonance D; (f) saturation of resonance E.

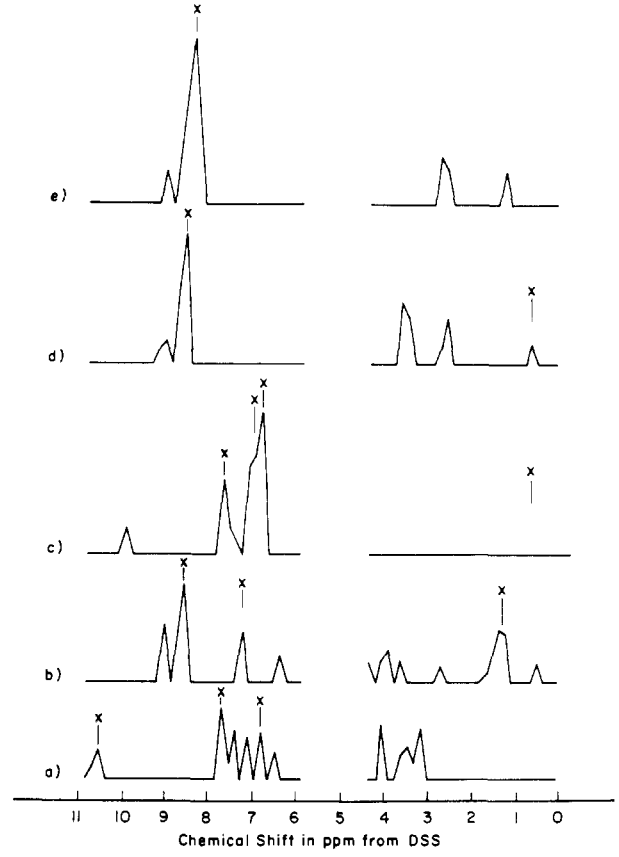

FIGURE 7: NOE action spectra for peaks A–E of reduced superoxide dismutase at pH 6.6 and 20 °C. The changes in intensities of peaks A–E are displayed as the difference between a control spectrum and an irradiated spectrum. These intensities are plotted vs. the preirradiation frequency which was varied between 0 and 11 ppm in steps of 40 Hz. The power of the preirradiation pulse was set to saturate roughly 50% on resonance, in order to avoid affecting an unacceptably wide region. The largest NOE's are 10–15%. NOE's previously observed from downfield to the central region are marked with an ×. (a) Peak A; (b) peak B; (c) peak C; (d) peak D; (e) peak E.

relaxation rate contains no contribution from solvent exchange. This indicates that magnetization transfer within the protein is rapid relative to the intrinsic relaxation of these protons. The dominant mechanism of saturation–recovery for the N protons must be cross relaxation with neighboring spins. We conclude that the substantial transfer of saturation from water to the histidine N protons probably occurs by protein proton-mediated cross relaxation.

The efficient cross relaxation demonstrated above suggested that specific nuclear Overhauser effects (NOE) might be observable. These NOE's are seen by selectively saturating a resonance while monitoring the rest of the protein spectrum for intensity changes. Difference spectra (spectra without irradiation minus spectra with irradiation) may show changes at resonances of protons which are within about 3.5 Å of the irradiated proton. NOE difference spectra for histidine NH resonances A–E are shown in Figure 6. A negative NOE is observed connecting each histidine NH resonance with a C2 proton resonating between 7.5 and 9.0 ppm from DSS. Negative NOE's to C4 protons resonating between 6.0 and 7.5 ppm are seen for three histidine N protons. In addition, specific negative NOE's are seen from proton A to a resonance at 10.46 ppm, tentatively assigned to a peptide N proton, and from peak C to a peak at 7.02 ppm. Protons B–D also show small effects in the aliphatic region. We have observed these NOE effects in at least three samples and they are reproducible.

The NOE's were confirmed in a complementary experiment where the histidine NH resonances were observed, while a semiselective preirradiation pulse was applied in other parts of the proton spectrum. Action spectra, in which the amplitudes of the NH resonances are plotted vs. the frequency of preirradiation, are shown in Figure 7. All NOE's seen previously (except one, peak C to a methyl proton) were confirmed in this experiment. In addition, several undetected effects were observed, but in all cases these were small and barely above the level of noise. The most prominent NOE's are summarized in Table II.

Table II: Summary of NOE Data[a]

proton	chemical shift[b] (ppm)	intensity (%)	possible assignments
A	10.46	12	peptide NH
A	7.71	17	C2–H
A	6.74	10	C4–H
B	8.62	~20	C2–H
B	7.23	~10	C4–H
B	1.31		CH_3 or CH_2
C	7.70	5	C2–H
C	7.02	7	C4–H
C	6.79	10	C4–H
C	0.64		CH_3
D	8.60	25	C2–H
D	0.62		CH_3
E	8.44	20	C2–H

[a] Conditions are as described in Figure 6. [b] In parts per million from DSS, assuming that the H_2O chemical shift is 4.82 ppm.

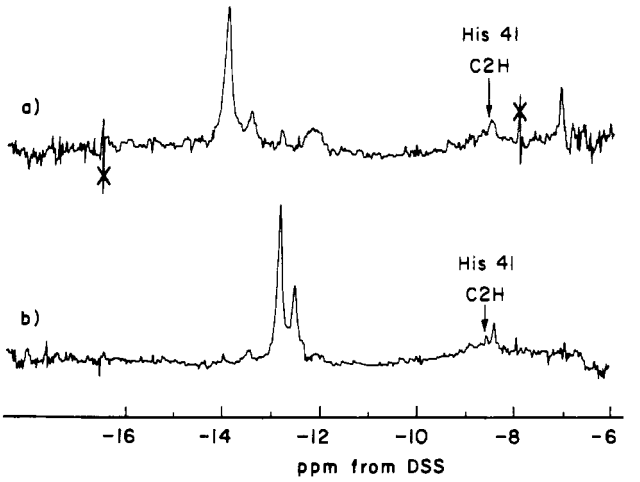

FIGURE 8: NOE difference spectra of resonances B and D of superoxide dismutase which has been deuterated at the C2 position of His-41 at pH 6.5 and 20 °C. The position of the His-41 C2–H NOE is marked. The small NOE seen is presumably due to unexchanged His-41 C2 protons. The ×'s mark unreproducible glitches. (a) Peak B; (b) peak D.

A histidine C2 proton, resonating near 8.6 ppm, which can be selectively exchanged for deuterium or tritium has been identified as the His-41 C2 proton (Cass et al., 1977a). Histidine N protons B and D both show NOE's at this chemical shift, suggesting that one or both are His-41 N protons. The His-41 C2 proton was selectively replaced by deuterium as described under Experimental Section. Examination of the NOE's of resonances B and D in the modified protein showed that both effects disappear (Figure 8). There are two possibilities: (1) protons B and D may be the N protons of protonated His-41 or (2) two C2 protons resonating at 8.6 ppm were both replaced with solvent deuterons under the conditions intended to exchange the His-41 C2 proton alone. We were careful to duplicate the procedure used previously (Cass et al., 1977a), where only one C2 proton was observed to exchange, and believe the first possibility is most likely.

As further confirmation, we looked for a secondary NOE between resonances B and D which is expected if both belong to His-41. Proton B shows approximately a 20% NOE to the C2 proton (Table II), and the C2 proton shows approximately a 10% NOE to proton D (Figure 7). Roughly a 2% NOE from resonance B to resonance D should be seen if both are His-41 protons. NOE's from proton B to proton D and from proton D to proton B of this approximate magnitude were observed (Figure 9), thus confirming the assignments of these protons. The fact that the putative NOE to peak D in parts b and c of Figure 9 is greater than the presumed spillover to direct irradiation on peak C shows that the NOE is not an artifact due to spillover.

Discussion

Assignments. Resonances B and C. We showed above that B and D can be assigned to the N3 and N1 protons of His-41. To summarize the evidence, both resonances show NOE's to the relatively rapidly exchanging C2 proton, which was previously identified as the His-41 C2 proton (Cass et al., 1977a), and the predicted secondary NOE between protons B and D has been observed. Resonance B must be assigned to the N3 proton because it shows NOE's to both a C2 and a C4 proton.

Resonances A and C. Resonances A and C show no evidence of pH titration or rapid chemical exchange, suggesting

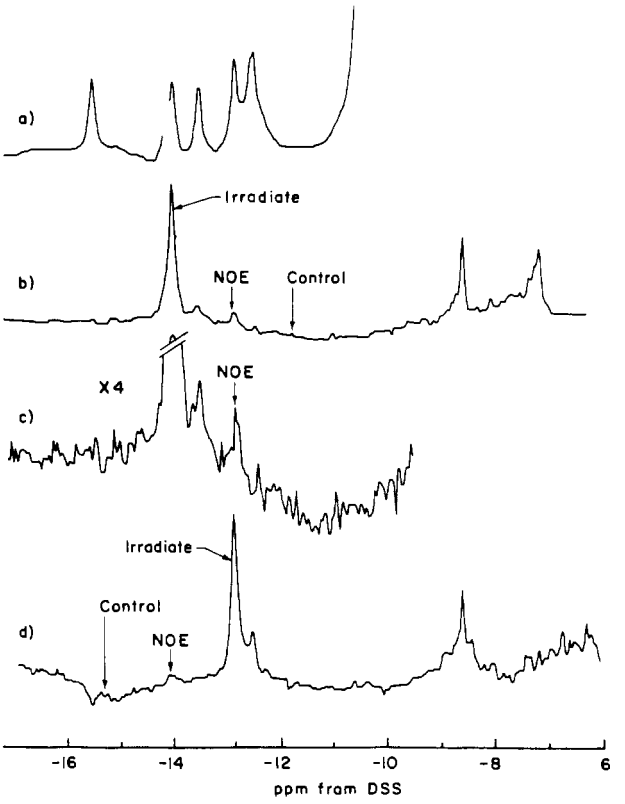

FIGURE 9: Difference spectra showing the secondary NOE between resonances B and D of reduced superoxide dismutase at pH 6.3 and 20 °C. The frequencies of the preirradiation pulses in the control and irradiated spectra were placed symmetrically about the position of the NOE to cancel out effects due to direct saturation. The amplitudes of the NOE's are 1–2%. (a) The downfield proton spectrum; (b) saturation of resonance B; (c) saturation of B at 4× gain; (d) saturation of resonance D.

they are due to metal-liganded histidine residues. The remaining unassigned nonactive-site histidine residue, His-19, is exposed to solvent and ionizes with a pK_a of 6.7 (Cass et al., 1977b). Its N protons would be expected to be broadened beyond detection by rapid chemical exchange at high pH values. Our assignment of resonances A and C depends on two observations: (1) the protons have very slow but nearly identical chemical exchange rates, suggesting they are highly inaccessible to solvent and/or strongly hydrogen bonded; (2) the protons show NOE's to both C2 and C4 protons, indicating the protons of interest are N3 protons. These residues are metal ligands, so this bonding must occur at the N1 position. Examination of the crystal structure shows that only two histidine residues fulfill these criteria. These are His-44, a copper ligand, and His-69, a zinc ligand. Both are almost certainly liganded to the metals at the N1 position (J. S. Richardson, personal communication). The remaining histidines appear to be liganded at the N3 position (except for His-61 which is liganded at both nitrogens and for His-78 where the liganding position is ambiguous). Residues 69 and 44 are completely buried and, of all histidines, these appear the least accessible to solvent. The N3 protons of both residues are hydrogen bonded to the carboxylate of Asp-122, providing explanation for their slow, but nearly identical, chemical exchange rates. While we are confident of our assignment of resonances A and C to His-44 or His-69, assignment of each resonance to a specific residue is more tentative. Proton A shows an NOE to a peptide N proton and proton C to what is probably an aromatic proton. The N3 of His-69 is near a peptide NH group in the crystal structure and the N3 of His-44 is near the C4 proton of His-61 so we will assign

resonance A to His-69 and resonance C to His-44. However, our results for these protons do not depend on this very tentative assignment.

Resonances E and F. Resonances E and F remain unassigned. Resonance E shows no evidence of pH titration or rapid chemical exchange at neutral pH and cannot be due to His-19. Possible assignments for this peak are the N1 protons of histidines-46, -61, -78, or -118. Resonance F may be from any of these residues or His-19.

Oxidized Enzyme. The most reasonable assignments for the two broad histidine NH resonances in the oxidized protein spectrum are the N1 and N3 protons of His-41. Both resonances show an NOE at 8.6 ppm (unpublished observations), which is the chemical shift of the His-41 C2 proton in the reduced enzyme (Cass et al., 1977a). The 13.8-ppm resonance also shows rapid chemical exchange behavior above pH 7 as was observed for the His-41 N3 proton in the reduced enzyme (resonance B). His-41 is about 12 Å from the Cu^{+2} atom (Cass et al., 1977b). Therefore, its NH resonances should be broadened but still visible. This is what is observed, so we assign the 13.8-ppm resonance to the His-41 N3–H and the 12.4-ppm peak to the His-41 N1–H.

NOE Distance Measurements. In principle, interproton distance determinations are possible from NOE data. A quantitative treatment in a macromolecule is complicated because of the large number of possible dipole–dipole interactions with surrounding spins. An approximation, based on a generalization of a two-spin interaction, appears to be adequate for many purposes, but the large number of NOE's and relaxation rates necessary for the calculation cannot be obtained. A qualitative analysis is possible if several additional approximations are made.

As outlined by Kalk & Berendson (1976), longitudinal relaxation of the magnetization of the ith spin, I_{zi}, due to dipolar interaction with neighboring spins is given by eq 2.

$$\frac{dI_{zi}}{dt} = -(R_{1i} + \sum_{j\neq i} R_{tij})(I_{zi} - I_{oi}) + \sum_{j\neq i} R_{tij}(I_{zj} - I_{oj}) \quad (2)$$

R_{1i}, the local spin–lattice relaxation rate of the ith spin, is given by eq 3. When other relaxation mechanisms are important, contributions from these will be included in R_{1i}. R_{tij}, the cross relaxation rate between spins i and j is given by eq 4.

$$R_{1i} = \frac{1}{10}\gamma^4\hbar^2\sum_j \frac{1}{r_{ij}^6}\left[\frac{3\tau_c}{1 + (\omega\tau_c)^2} + \frac{12\tau_c}{1 + (2\omega\tau_c)^2}\right] \quad (3)$$

$$R_{tij} = \frac{1}{10}\frac{\gamma^4\hbar^2}{r_{ij}^6}\left[\tau_c - \frac{6\tau_c}{1 + (2\omega\tau_c)^2}\right] \quad (4)$$

In these equations, τ_c is the correlation time for the dipolar coupling between spins i and j, r_{ij} is the distance between spins i and j, and ω is the Larmor frequency. The magnitude of the equilibrium NOE on spin i observed when spin k is saturated can be obtained from eq 2 by letting $dI_{zi}/dt = 0$ and assuming the magnetizations of all spins, except i and k, are equal to their equilibrium value. We thus ignore possible secondary NOE effects arising from interaction with a third spin. This yields

$$\frac{I_{zi} - I_{oi}}{I_{ok}} = \frac{R_{tik}}{R_{1i} + \sum_{j\neq i} R_{tij}} \quad (5)$$

The approximation concerning second order NOE's is not rigorously justified, but, to minimize errors, relatively short saturation pulses ($\sim 2T_1$) were used in our NOE experiments. As a result, the amplitudes we report will tend to be smaller than the true equilibrium NOE's.

Additional approximations are required to obtain interproton distances from eq 5. The rate of magnetization recovery after selective saturation will be the sum of the intrinsic relaxation rate and all cross relaxation processes ($R_{1i} + \sum_{j\neq i} R_{tij}$). Therefore, we can replace the sum in the denominator of the right-hand side of eq 5 with the saturation–recovery rate T_{1a}^{-1}. Unfortunately, this rate was not measured for the aromatic, amide, and methyl protons. A direct measurement of T_{1a} for these protons is impossible because their resonances are not resolved. Their T_{1a} can be estimated accurately enough by studying the NOE as a function of irradiation time after an adequate recovery time, and such measurements have been performed on hemoglobin and transfer RNA (T.-H. Huang, J. S. Tropp, and A. G. Redfield, unpublished experiments), but we did not have time to do so in the present case. T_{1a} was measured directly for the imidazole N protons, but only the lower limit of size of the NOE to these protons was known (Figure 7) because we could only estimate the degree of saturation in the action spectra. Thus, no precise value for R_{tik} could be inferred from our data from any pair of spins. As a first approximation, we estimated this rate from the N to the C2 and C4 protons by assuming that the latter had a T_{1a}^{-1} equal to that of the N proton ($\sim 20\ s^{-1}$). Equation 4 and an estimate of τ_c from Stokes law for rotational diffusion ($\sim 1 \times 10^{-8}$ s) can then be used to determine interproton distances from the R_{tik} values.

Histidine N to C2 proton distances calculated this way vary from 2.3 to 2.8 Å for peaks A–E. Alternately, using the largest C2–H to NH NOE, which is a lower limit on the true equilibrium NOE, and the known C2–H to NH distance of about 2.5 Å, the correlation time, τ_c, for the dipolar coupling can be obtained. A τ_c value of 1.8×10^{-8} s is found which compares favorably with the lower limit calculated from the Stokes equation. This τ_c value can be used with other NOE data to determine unknown interproton distances. For example, the distance between peak A and the peptide NH proton is estimated to be 2.8 Å. Our results are based on several approximations and should be considered qualitative. The good agreement obtained between calculated and known distances is in large part due to the inverse sixth power distance dependence of the dipolar coupling which minimizes errors. We can reliably estimate that, for superoxide dismutase (M_r 31 200), two protons must be within 4.0 Å of each other for a measurable primary NOE to occur. This treatment has not considered secondary (three-spin) NOE effects. These may give rise to measurable NOE's for protons more than 4.0 Å apart.

Histidine Environments. We have assigned the ring protons of three histidine residues and would like to discuss the environments of each residue as revealed by the NMR and the crystallographic results.

His-41. Two N protons are observed from His-41 below pH 7.5. Above this pH, the N3–H resonance is broadened beyond detection by chemical exchange. However, the chemical shift of the N1–H resonance is pH independent until near pH 10. This resonance shifts upfield with a pK_a of ~ 10.4, probably due to deprotonation of the N3 position. This pK_a is 3 or 4 units higher than normal and corresponds to about 5 kcal of free energy stabilization of the protonated imidazole ring. Examination of the crystal structure shows that His-41 is involved in a salt bridge with the Glu-119 carboxylate at one nitrogen position and may form a weaker interaction with the Asp-40 carboxylate at the other nitrogen position (J. S.

Richardson, personal communication). Considering these interactions, the pK_a shift observed is reasonable. For example, the pK_a of an α-amino group in chymotrypsin is observed to shift more than 2 units because it forms an ion pair with a nearby Asp residue (Fersht, 1972).

The unusually fast chemical exchange observed for the C2 proton of this residue is also consistent with our interpretation. Hydroxide-catalyzed exchange of an imidazole C2 proton proceeds through a carbanion intermediate at the C2 position. A positive charge on the nitrogen atoms stabilizes this carbanion and increases the rate of exchange (Matsuo et al., 1972; Harris & Randall, 1965; Vaughan et al., 1970). His-41 remains protonated to an abnormally high pH, and, therefore, exchange occurs more rapidly for the C2 proton of His-41 than for the other His residues.

The role the Glu-119–His-41–Asp-40 interaction plays in the structure and function of superoxide dismutase is not known, although a structural role seems likely. The properties of the carboxylate–imidazolate pair (solvent exchange rates, pK_a values, etc.) are very different from the properties of the carboxylate–imidazolate pair of the charge-relay system of the serine proteases (Markley & Ibânez, 1978). It is not clear how other parts of the structure affect these properties and additional study is warranted.

His-44 and His-69. The solvent exchange rates of the N3 protons of His-44 and His-69 are reduced by 6–7 orders of magnitude relative to that of free histidine. Some of this rate decrease is due to solvent inaccessibility, but much is probably due to the hydrogen bond each residue forms with the Asp-122 side-chain carboxylate. Superoxide dismutase has three distinct structural features: an eight-stranded, cylindrical β barrel and two long loops of nonrepetitive structure (Richardson et al., 1975a). The metal-binding sites are on the exterior of the β barrel, which contributes four ligands. The loops contribute the remaining three ligands and complete the binding cavity. His-44 is a β-barrel residue, His-69 is on one of the loops, and Asp-122 is on the other loop, so the interaction between them would seem important to maintenance of the tertiary structure of the metal-binding sites. The hydrogen-bonded NH protons should be good indicators of the structural integrity of this part of the molecule even if the interaction is not important energetically. The remarkably slow solvent exchange is strong evidence for a rigid structure, with few conformational fluctuations which would permit the solvent accessibility necessary for exchange.

Similar exchange rates and activation energies are observed for both N protons, suggesting they have similar solvent exchange mechanisms. However, the rates and activation energies are not identical. Thus, these two N protons are not exchanging with each other on a time scale rapid compared to the exchange of the faster one (resonance A) with solvent. It is conceivable that the slower proton C first moves to site A and then to solvent, but this would require similar rates for two rather different processes, namely, C to A interchange and A to solvent exchange. The ~30-kcal activation energy observed for both exchanges seems too small to be associated with a major rearrangement of the protein, and, therefore, it may be associated with a relatively simple rate-determining step such as transfer to a relatively mobile water molecule.

The C2 protons of His-44 and His-69 have chemical shifts characteristic of deprotonated histidine (7.7 ppm). Histidine residues which are liganded to metals are expected to show chemical shifts near 8.0 ppm, characteristic of doubly protonated histidines (Sugiura, 1977; Temussi & Vitagliano, 1975). The smaller chemical shift in the protein may reflect the true net charge of these histidine residues and may imply either that the metal–histidine bonding is relatively weak or that the negatively charged Asp-122 carboxylate reduces the partial positive charge on the imidazole ring.

Acknowledgments

We thank Dr. I. Fridovich for his support and encouragement and Drs. J. S. Richardson and D. C. Richardson for access to their 2-Å resolution electron density map of superoxide dismutase and for permitting us to quote some of their preliminary results.

References

Beem, K. M., Richardson, D. C., & Rajagopalan, K. V. (1977) *Biochemistry 16*, 1930.

Cass, A. E. G., Hill, H. A. O., Smith, B. E., Bannister, J. V., & Bannister, W. H. (1977a) *Biochem J. 165*, 587.

Cass, A. E. G., Hill, H. A. O., Smith, B. E., Bannister, J. V. & Bannister, W. H. (1977b) *Biochemistry 16*, 3061.

Fersht, A. R. (1972) *J. Mol. Biol. 64*, 497.

Fridovich, I. (1975) *Annu. Rev. Biochem. 44*, 147.

Glickson, J. D., Rowan, R., Pitner, T. P., Dadok, J., Bothner-by, A. A., & Waller, R. (1976) *Biochemistry 15*, 1111.

Harris, T H., & Randall, J. C. (1965) *Chem. Ind. (London)*, 1728.

Kalk, A., & Berendson, H. J. C. (1976) *J. Magn. Reson. 24*, 353.

Lippard, S. J., Burger, A. R., Ugurbil, K., Pantoliano, M. W., & Valentine, J. S. (1977) *Biochemistry 16*, 1136.

Markely, J. L., & Ibânez, I. B. (1978) *Biochemistry 17*, 4627.

Matsuo, H., Ohe, M., Sakiyama, F., & Nanita, K. (1972) *J. Biochem. (Tokyo) 27*, 1057.

McCord, J. M., & Fridovich, I. (1969) *J. Biol. Chem. 244*, 6049.

Redfield, A. G., Kunz, S. D., & Ralph, E. K. (1975) *J. Magn. Reson. 19*, 114.

Richardson, J. S., Thomas, K. A., Rubin, B. H., & Richardson, D. C. (1975a) *Proc. Natl. Acad. Sci. U.S.A. 72*, 1349.

Richardson, J. S., Thomas, K. A., & Richardson, D. C. (1975b) *Biochem. Biophys. Res. Commun. 63*, 986.

Stoesz, J. D., Redfield, A. G., & Malinowski, D. (1978) *FEBS Lett. 91*, 320.

Sugiura, Y. (1977) *Eur. J. Biochem. 78*, 431.

Temussi, P. A., & Vitagliano, A. (1975) *J. Am. Chem. Soc. 97*, 1572.

Vaughan, J. D., Mughrabi, Z., & Wu, E. C. (1970) *J. Org. Chem. 35*, 1141.